Novel Bifunctional Quinolonyl Diketo Acid Derivatives as HIV-1 Integrase Inhibitors: Design, Synthesis, Biological Activities, and Mechanism of Action

Roberto Di Santo,*,† Roberta Costi,† Alessandra Roux,† Marino Artico,† Antonio Lavecchia,*,‡ Luciana Marinelli,‡ Ettore Novellino,‡ Lucia Palmisano,§ Mauro Andreotti,§ Roberta Amici,§ Clementina Maria Galluzzo,§ Lucia Nencioni,|| Anna Teresa Palamara,|| Yves Pommier,⊥ and Christophe Marchand⊥

Istituto Pasteur−Fondazione Cenci Bolognetti, Dipartimento di Studi Farmaceutici, and Istituto di Microbiologia, Università di Roma "La Sapienza", P. le A. Moro 5, I-00185 Roma, Italy, Dipartimento del Farmaco, Istituto Superiore di Sanità, Viale Regina Elena 299, I-00161 Roma, Italy, Dipartimento di Chimica Farmaceutica e Tossicologica, Università di Napoli "Federico II", via D. Montesano 49, I-80131 Napoli, Italy, and Laboratory of Molecular Pharmacology, Center for Cancer Research, National Cancer Institute Building 37, Room 5068, National Institutes of Health, Bethesda, Maryland 20892-4255

Received November 18, 2005

The virally encoded integrase protein is an essential enzyme in the life cycle of the HIV-1 virus and represents an attractive and validated target in the development of therapeutics against HIV infection. Drugs that selectively inhibit this enzyme, when used in combination with inhibitors of reverse transcriptase and protease, are believed to be highly effective in suppressing the viral replication. Among the HIV-1 integrase inhibitors, the β-diketo acids (DKAs) represent a major lead for anti-HIV-1 drug development. In this study, novel bifunctional quinolonyl diketo acid derivatives were designed, synthesized, and tested for their inhibitory ability against HIV-1 integrase. The compounds are potent inhibitors of integrase activity. Particularly, derivative **8** is a potent IN inhibitor for both steps of the reaction (3′-processing and strand transfer) and exhibits both high antiviral activity against HIV-1 infected cells and low cytotoxicity. Molecular modeling studies provide a plausible mechanism of action, which is consistent with ligand SARs and enzyme photo-cross-linking experiments.

Introduction

Three different classes of chemotherapeutic agents are actually used to inhibit the replication of HIV-1, the etiological agent of acquired immunodeficiency syndrome (AIDS): the nucleoside (NRTI) and non-nucleoside (NNRTI) reverse transcriptase inhibitors, the protease inhibitors (PRI), and the inhibitors of the fusion of the virus with the host cell (for review, see ref 1). The highly active anti-retroviral therapy (HAART), which is based on the use of a combination of the cited drugs, effectively inhibits the replication cycle of HIV-1. The advent of HAART has made possible the suppression of the HIV-1 replication to such an extent that the virus becomes undetectable in the blood of infected persons. As a consequence, a decline of both mortality and morbidity due to the HIV-1 was reported in the recent years. However, HAART fails to eradicate viral replication, which persists at a low level in cellular reservoirs, despite the chemotherapy.[2] The ability of HIV-1 to evolve drug resistance and the toxicity of HAART regimens make integrase (IN), which is the third virally encoded enzyme required for HIV-1 replication, a legitimate target for the development of new drugs. Moreover, IN has no cellular counterpart, and thus came into sight 10 years ago as a new therapeutic opportunity.[3−6] Hopefully, integrase inhibitors will become a potential additive to HAART or a salvage therapy for patients resistant to currently available anti-HIV drugs.

IN catalyzes the insertion of viral DNA into the host genome derived from reverse transcription of HIV RNA. Integration occurs via a multistep sequence of reactions, including (i) cleavage of a dinucleotide pair from the 3′-end of the viral DNA (termed "3′-processing", 3′-P), (ii) insertion of the resulting shortened strands into the host-cell chromosome (termed "strand transfer", ST), and (iii) removal of the two unpaired nucleotides at the 5′-end of the viral DNA and gap-filling process (for review, see ref 6).

Numerous compounds with different structural features have been reported as IN inhibitors[6,7] of which the most important class is typified by an aryl β-diketo acid motif (DKAs)[8] (compound **1**,[9] Figure 1). DKAs selectively inhibit the ST reaction of IN and exhibit antiviral activity against HIV-1-infected cells in a manner consistent with inhibition of integration.[8,10] These compounds are also useful tools to explore the molecular mechanism of IN.[8,11,12]

More recently, some bifunctional DKAs (BDKAs) were reported, which are characterized by the presence of two diketo acid chains in the skeleton of the IN inhibitor (compounds **2**−**4**, Figure 1).[13−15] However, the BDKAs reported so far were less potent than mono functional counterparts and endowed with low antiviral activities. These properties could be ascribed to the lack of some important structural features in the reported BDKAs. In fact, structure−activity relationships on monofunctional aryl diketo acids led to the conclusion that the highest activity was obtained when the central aromatic ring is 1,3-disubstituted with the diketo acid chain and a benzyl moiety (see compound **1**, Figure 1). In such a way, the angle between the two lines extended from the above groups is around 120°.[9]

The aim of the present work was to obtain new BDKAs with improved activity against IN and HIV-1-infected cells. Thus, on the basis of our prior experience,[16] we designed new

* To whom correspondence should be addressed. R.D.S.: phone and fax, +39-6-49913150; e-mail, roberto.disanto@uniroma1.it. A.L.: phone and fax, +39-81-678613; e-mail, lavecchi@unina.it.

† Dipartimento di Studi Farmaceutici, Istituto Superiore di Sanità.

‡ Dipartimento di Chimica Farmaceutica e Tossicologica, Università di Napoli "Federico II".

§ Dipartimento del Farmaco, Instituto Superiore di Sanità.

|| Istituto di Microbiologia, Università di Roma "La Sapienza".

⊥ Laboratory of Molecular Pharmacology, National Cancer Institute.

10.1021/jm0511583 CCC: $33.50
Published on Web 02/17/2006

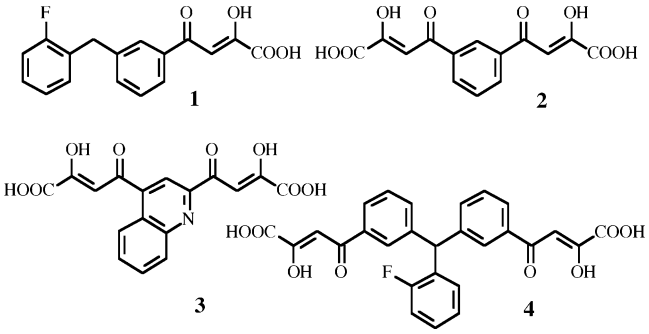

Figure 1. Structures of selected HIV-1 IN inhibitors belonging to the mono and bifunctional DKAs.

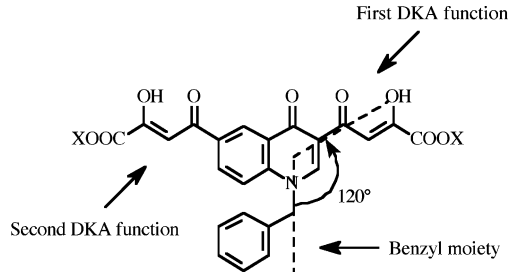

Figure 2. Structural features of the newly designed bifunctional quinolonyl diketo acid derivatives.

inhibitors **5**−**8** based on the 4-(4(1*H*)-quinolinon-3-yl)-2,4-dioxobutanoic acid skeleton (Figure 2). This scaffold was chosen because (i) it is easy to alkylate the 4(1*H*)-quinolinone at 1-position with a benzyl group to obtain a 1,3-disubstituted compound that well fits the geometric requirements for an optimal IN inhibitory activity and (ii) a second diketo acid function can readily be introduced at position 6 of the aromatic ring via an acetyl intermediate. Moreover, with the aim to characterize the mode of binding of the novel compounds within the IN, docking studies were performed and a molecular basis of enzyme inhibition is proposed.

Results and Discussion

Chemistry. The synthesis of derivatives **5**−**8** is outlined in Scheme 1. The key intermediate, 3,6-diacetyl-4(1*H*)-quinolinone (**9**), was obtained by reaction of 4-acetylaniline with ethyl ethoxymethyleneacetoacetate, followed by thermic cyclization in diphenyl ether. **9** was then alkylated with 4-fluorobenzyl bromide in alkaline medium (K_2CO_3) to afford *N*-1 substituted quinolinone **10**. Acetyl derivatives **9** and **10** underwent Claisen condensation with diethyl oxalate in the presence of sodium ethoxide as a catalyst to afford the diketo esters **5** and **7**, which were in turn hydrolyzed with 6 N NaOH to the corresponding acid derivatives **6** and **8**. The chemical and physical data of compounds **5**−**10** are reported in the Experimental Section; the spectroscopic data of derivatives **5**−**8** are given in the Supporting Information.

Evaluation of Biological Activities. In Vitro Assays. Derivatives **5**−**8** were tested in vitro for ST inhibition in the presence of magnesium (Mg^{2+}) using a novel electrochemiluminescent assay to generate IC_{50} values from triplicate experiments (Table 1). Compounds **5**−**8** were also tested for ST and 3′-P using gel-based assays in the presence of Mg^{2+} or Mn^{2+} (Figure 3). IC_{50} values were calculated using dose−response curves (Figure 3B,C) and are summarized in Table 1. The newly synthesized BDKAs exhibit potent inhibitory activity against IN for both ST and 3′-P steps. The acid derivatives (**6**, **8**) are more potent than the corresponding esters (**5**, **7**), and the 1-*p*-F-benzyl-substituted quinolinones (**7**, **8**) are more active than the unsubstituted counterparts (**5**, **6**). Derivative **8** is the most potent derivative with IC_{50} values for strand transfer around 15 nM (Figure 3 and Table 1). Compound **8** is selective for ST inhibiton with IC_{50} values approximately 20-fold lower for ST than for 3′-P (Figure 3, compare panels B and C; Table 1). Compound **8** also inhibits integrase with similar potency in the presence of Mg^{2+} or Mn^{2+} (Table 1). The activity in the presence of Mg^{2+} in addition to the selectivity for ST represents a trademark of the most potent DKAs.[11] Compound **8** is to our knowledge, the most potent bifunctional diketo acid derivative reported to date.

Scheme 1[a]

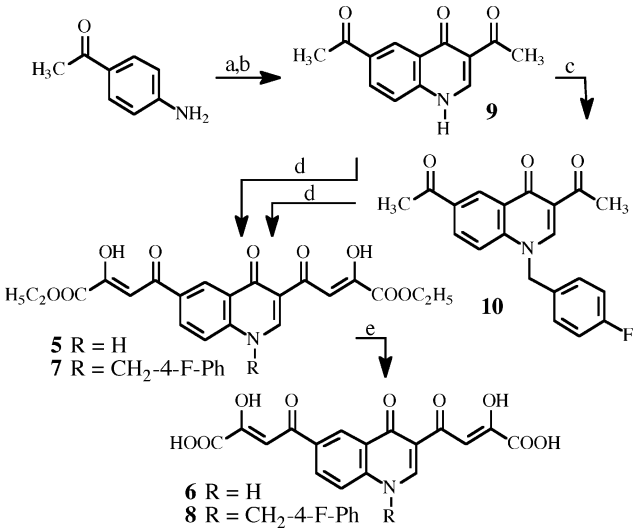

[a] Reagents and conditions: (a) ethyl ethoxymethyleneacetoacetate, neat, 120 °C 5 min, 73%; (b) Ph_2O, reflux 50 min, 56%; (c) 4-flurobenzyl bromide, K_2CO_3, DMF, reflux 2 h, 88%; (d) diethyl oxalate, C_2H_5ONa, THF·C_2H_5OH, rt 2 h, **5** (100%), 45 min, **7** (88%); (e) 1 N NaOH, rt 1.5 h, **6** (52%), **8** (77%).

Cell-Based Assay. Antiviral activities are presented in Table 1. Compound **8** showed good antiviral efficacy in HIV-1-infected H9/HTLVIIIB cells ($EC_{50} = 4.29\ \mu M$, $EC_{90} = 40\ \mu M$) and low cytotoxicity ($CC_{50} > 200\ \mu M$, SI > 46.6). **6** and **7** were 8 and 5 times, respectively, less potent than the parent compound **8**, while **5** was inactive below 50 μM concentration. Note that the quinolonyl derivative **8** showed higher potency in inhibiting the replication cycle of HIV-1 in cell-based assays (EC_{50}) and better SI than the reference derivatives **3** and **4**.

These structure−activity relationships emphasize the relevance of the free carboxylic acid group and the *p*-F-benzyl moiety for both tight binding with IN and high antiviral potency.

Docking Studies. To elucidate the binding mode of the most active compound (**8**) within the IN catalytic core domain (CCD), docking calculations were carried out using the X-ray structure 1BIS (subunit B).[17] A Mg^{2+} ion, was placed in the active site between the carboxylate oxygen atoms of residues D64 and D116, considering the geometry of the Mg^{2+} ion present in the PDB structure 1QS4 (subunit A).[18]

To take into account protein flexibility, **8** was docked to an ensemble of protein snapshots taken from a 1-ns molecular dynamics (MD) simulation, according to the relaxed-complex method.[19] The program AutoDock 3.0.5 was chosen because it utilizes a fully flexible ligand in its docking algorithm and because it has been shown to successfully reproduce many crystal structure complexes.[20] Details of the docking setup and the MD simulation protocol are provided as Supporting Information. The protein turned out to be very stable throughout the

Table 1. Cytotoxicity and Antiviral and Anti-Integrase Activities of Derivatives **5**−**8**

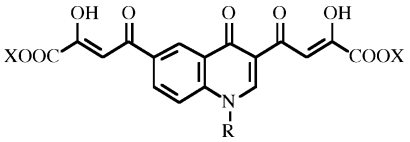

			anti-IN activity: IC_{50}[a]							
			ST			3′-P		antiviral activity		
compd	R	X	Mg^{2+} [b]	Mg^{2+} [c]	Mn^{2+} [c]	Mg^{2+} [c]	Mn^{2+} [c]	CC_{50}[d]	EC_{50}[e]	SI[f]
5	H	C_2H_5	77 ± 13	39	80	28	>333	>200	>50	–
6	H	H	9.1 ± 1.2	2.9	0.43	22	>4.1	>200	36.3	5.5
7	Bz[g]	C_2H_5	0.38 ± 0.01	0.29	0.25	21	40	191	20	9.6
8	Bz[g]	H	0.016 ± 0.004	0.017	0.012	0.44	0.20	>200	4.29[h]	>47
2[i]					1.83		7.8	nr[j]	nr	–
3[i]					6.5		82	>25	61[k]	–
4[i]					0.2		1.8	81	17	4.8

[a] Inhibitory concentration 50% (μM) determined from dose−response curves. [b] Experiments performed in triplicate using the BioVeris assay (ST assay in the presence of $MgCl_2$). [c] Experiments performed on gels in the presence of $MnCl_2$ or $MgCl_2$ (see Figure 3). [d] Cytotoxic concentration 50% (μM). [e] Effective concentration 50% (μM). [f] Selectivity index = CC_{50}/EC_{50}. [g] Bz = CH_2-4-F-Ph. [h] For this compound, EC_{90} = 40 μM was determined. [i] Literature data; see refs 11−13. [j] nr: not reported. [k] Percentage of inhibition obtained at a concentration of 25 μM.

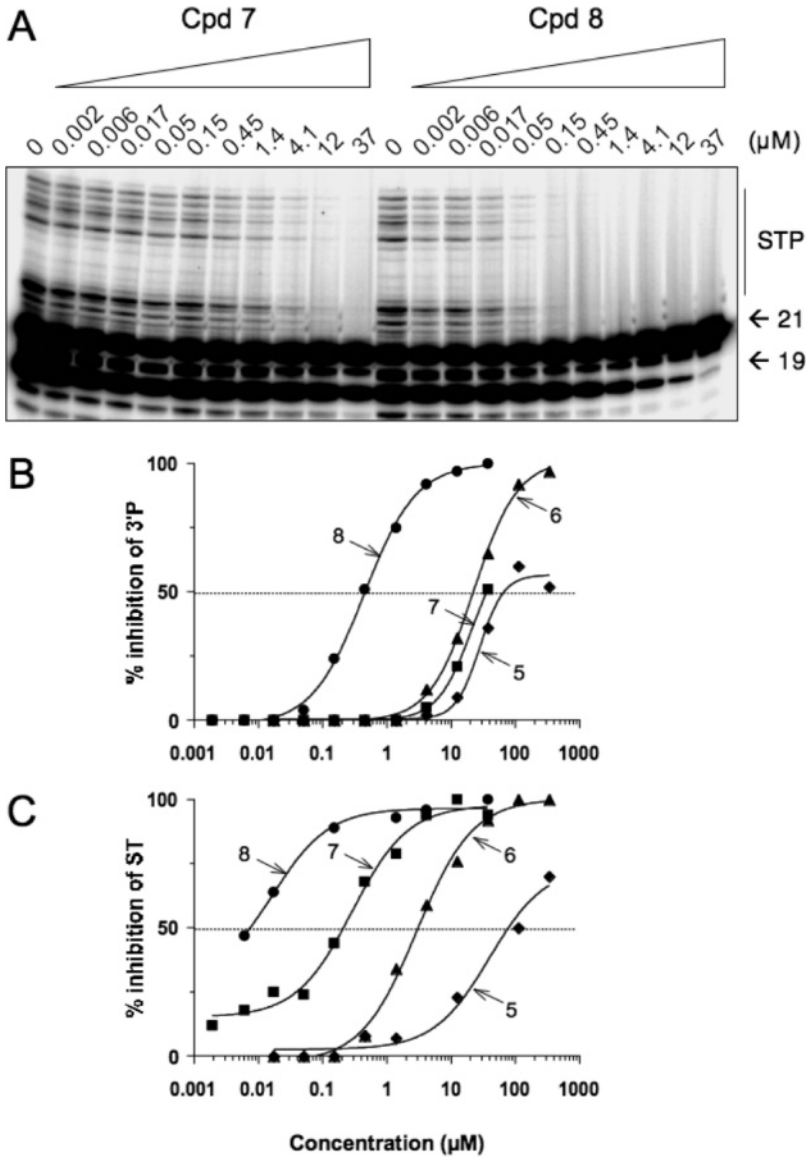

Figure 3. Comparison of HIV-1 integrase inhibition by compound **7** and **8** in the presence of Mg^{2+}. (A) Phosphorimager image showing a representatitve experiment. 21, 19, and STP correspond to DNA substrate, 3′-processing product, and strand transfer products, respectively. (B) HIV-1 integrase inhibition curve (derived from densitometric analysis of typical experiments) for 3′-processing. (C) HIV-1 integrase inhibition curve for strand transfer.

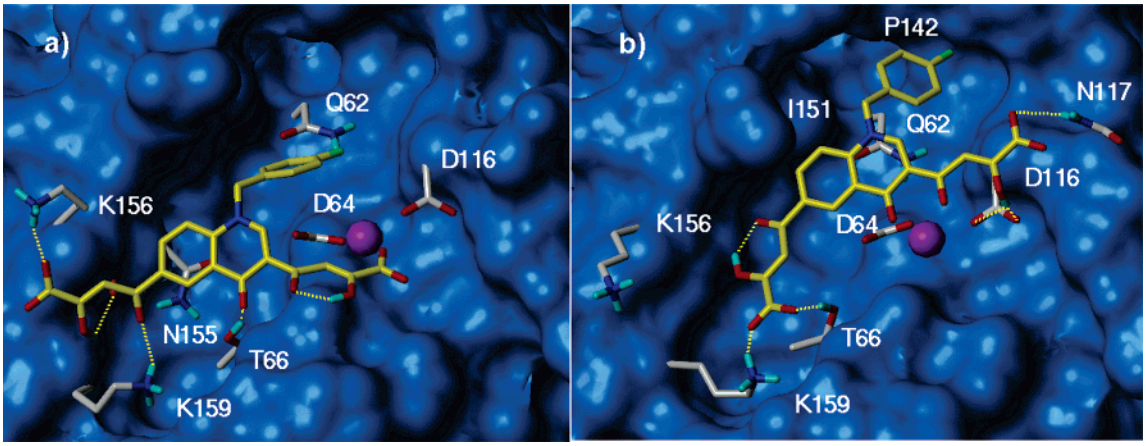

Figure 4. The two predominant binding modes of **8** (yellow) to MD snapshots of the IN core domain. Residues lining the ligand position are highlighted. The metal ion is represented as a magenta sphere.

MD simulation, with the exception of the three loop regions 139−147, 165−172, and 185−196. The former, which we refer to as "catalytic loop" is located close to the active site. Its importance for the catalytic activity together with the flexible nature are well-known.[21] According to previous MD studies, the catalytic loop moves back and widens the active site region.[22] The Mg^{2+} coordination by D64 and D116 residues was always conserved during the production run.

Docking of **8** to the MD snapshots, collected every 100 ps, revealed two predominant binding modes, which are shown in Figure 4. In the binding orientation shown in Figure 4a, the carboxylate group of one diketo acid chain of the ligand chelates the Mg^{2+} metal ion, whereas the other one inserts between residues K156 and K159, forming H-bonds with both side chains and with N155 CO backbone. The *p*-F-benzyl group points toward a hydrophobic pocket formed by the catalytic loop residues Y143, P142, I141, and G140 and by residues I60, Q62, V77, V79, H114, G149, V150, I151, E152, S153, and M154. Particularly, a favorable electrostatic interaction occurs between the fluorine atom on the benzyl ring and the amide group of Q62 residue. The quinoline ring of the molecule forms a stacked amide−aromatic interaction with the N155 side chain, while the quinoline carbonyl oxygen enables a hydrogen bond to the T66 side chain. In our model, T66, S153, and M154, whose mutations were found to confer resistance to DKAs, are all in close proximity of the ligand.[8]

A significant alternative to the described binding mode is given by a docking position in which the metal ion is chelated in a bidentate manner by the quinoline carbonyl oxygen and by one oxygen of the diketo acid function, while the hydroxyl and the carboxylate groups of the same branch contact the D116 and the N117 side chains, respectively (Figure 4b). On the opposite side of the molecule, the other diketo acid arm elongates toward the K156 and K159 residues contacting exclusively the latter amino acid. The *p*-F-benzyl group entirely inserts in the hydrophobic pocket, where it is stabilized by hydrophobic interactions with I151 and P142 side chains. Although the two binding modes differ in some details, it is worth noting that, in both docking solutions, the ligand interacts with the same enzyme attachment points: (i) the metal ion, (ii) the K156 and/or K159 residues, and (iii) the hydrophobic pocket.

The reduced inhibitory potencies of diketo esters **5** and **7** compared to their respective acids **6** and **8** is due to the ability of both carboxylic functionalities to chelate the metal ion and to interact with the above-mentioned lysine residues, whereas the diketo esters weakly bind to these portions of the enzyme.

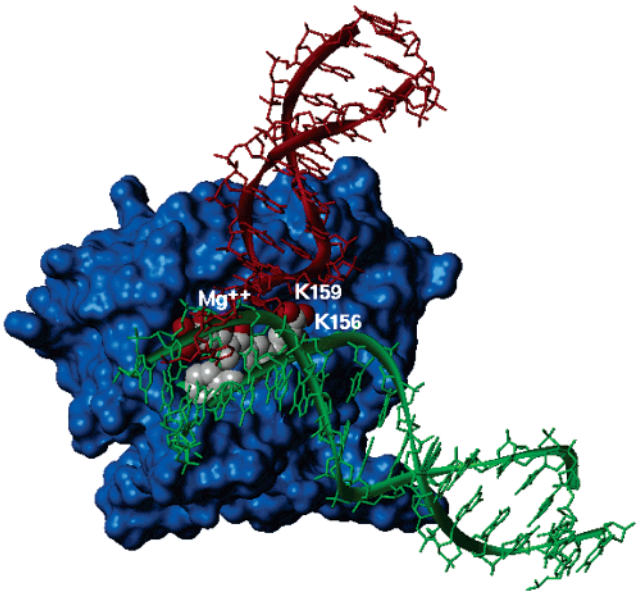

Figure 5. Model of IN CCD−DNA complex with **8** (rendered as CPK) bound to the active site. Donor DNA is in red and acceptor DNA is in green.

Thus, the free carboxylic functions are necessary for a strong interaction with the IN enzyme, particularly the metal ion. On the other hand, the drop in activity of **6** compared to **8** in both ST and 3′-P (see Table 1) can be clearly attributed to the absence of the *p*-F-benzyl moiety, which in our model inserts into the hydrophobic pocket, leading to a more efficient binding.

According to previous findings on BDKAs activity,[13] **8** is effective on both ST and 3′-P processes catalyzed by HIV-1 IN and in this feature differs from the reported monofunctional DKAs, which are generally found to be selective toward the ST. In this respect, it was hypothesized that BDKAs can bind both DNA acceptor and donor site of HIV-1 IN, being inhibitors of both ST and 3′-P processes, whereas the monofunctional DKAs selectively bind the acceptor site, being effective on ST.[13] Here, in an effort to gain more insight into the mechanism of action of the reported ligands, a re-evaluation of the above-described docking results was performed with the aid of the theoretical model of HIV-1 IN tetramer complexed with both donor and acceptor DNA developed by McCammon et al.[23] A visual inspection of **8** docked into the CCD−DNA complex (Figure 5) led us to the following considerations: (i) the diketo acid arm, which coordinates the Mg^{2+} metal ion, is clearly important in anchoring the ligand to the catalytic site. It is worth

noting that while this arm seems not to interfere with the donor DNA binding, it may physically hamper the acceptor DNA binding. In our model, either the acceptor DNA or the ligand contact the N117 residue (see Figure 4b). This amino acid plays a crucial role in the enzyme function as its mutation leads to an IN preferentially defective in the ST step of integration.[24] (ii) The other diketo acid function, inserting between K156 and K159 residues, would interfere with the donor DNA recognition and binding. This result is in accordance with photo-cross-linking data, which reveal that the above-mentioned lysines are critical for donor DNA binding.[25] This could explain the ability of **8** to inhibit the IN catalyzed 3′-P reaction. (iii) The *p*-F-benzyl group, which inserts in the hydrophobic pocket, would reduce the catalytic loop mobility and physically hamper the binding of the acceptor DNA. In the proposed model, both DNA molecules are in proximity of the loop; particularly, the acceptor DNA is in close contact with I151 and P142, which contribute to the ligand binding (Figure 4b). This finding also makes sense with respect to the experimental observation that the benzyl group in DKAs ligands is the primary determinant of the ST inhibition.[13]

Conclusions

We have designed, synthesized, and tested in both enzyme- and cell-based assays novel BDKAs as anti-HIV-1 agents targeted to IN. These compounds are potent inhibitors of both the ST and 3′-P steps and are endowed with antiviral activity. Docking experiments have helped to provide a framework for interpreting the inhibitory activity of our BDKAs. As more information becomes available to better characterize the details of DNA−IN interaction, this issue will be resolved more definitively. Moreover, studies on monofunctional derivatives related to **5**−**8** are in progress, with the aim to elucidate differences in the mechanisms of action.

Experimental Section

Chemistry. General. Melting points were determined with a Buchi 530 capillary apparatus and are uncorrected. Infrared (IR) spectra were recorded on a Spectrum-one spectrophotometer. ^{1}H NMR spectra were recorded on a Bruker AC 400 spectrometer. Merck silica gel 60 F_{254} plates were used for analytical TLC. Column chromatographies were performed on silica gel Merck 70−230 mesh. Concentration of solutions after reactions and extractions involved the use of a rotatory evaporator operating at a reduced pressure of approximately 20 Torr. Analytical results agreed to within ±0.40% of the theoretical values.

2-[[(4-Acetylphenyl)amino]methylene]-3-oxobutanoic Acid Ethyl Ester. A mixture of 4-aminoacetophenone (2.0 g, 0.015 mol) and 2-(ethoxymethylene)-3-oxobutanoic acid ethyl ester[26] (2.8 g, 0.015 mol) was heated at 120 °C for 5 min. After cooling, the solid that formed was washed with *n*-hexane and with a small amount of cold $CHCl_3$ to obtain pure 2-[[(4-acetylphenyl)amino]methylene]-3-oxobutanoic acid ethyl ester (3.0 g, 73%), mp 156−158 °C (benzene), which was used in the next reaction without further purification.

3,6-Diacetyl-4(1*H*)-quinolinone (9). 2-[[(4-Acetylphenyl)amino]-methylene]-3-oxobutanoic acid ethyl ester (5.0 g, 0.018 mol) was dissolved in boiling diphenyl ether (50 mL) and refluxed for 50 min. After cooling, the mixture was treated with *n*-hexane (100 mL) and the precipitate that formed was collected and filtered on a short silica gel column (ethyl acetate and then chloroform/methanol 10:1 as eluent) to afford **9** (2.3 g, 56%); mp >300 °C (DMF/water).

3,6-Diacetyl-1-(4-fluorophenylmethyl)-4(1*H*)-quinolinone (10). A solution of **9** (250 mg, 1.1 mmol) in dry DMF (10 mL) was treated with anhydrous K_2CO_3 (210 mg, 1.5 mmol) and 4-fluorophenylmethyl bromide (610 mg, 3.3 mmol) and the resulting suspension was stirred for 2.5 h at 100 °C. After cooling, cold water (0−4 °C) was added (40 mL) and the precipitate was filtered, washed with water and light petroleum ether in turn and then dried under an IR lamp to provide **10** (330 mg, 89%); mp 213−214 °C (toluene).

General Procedure for the Synthesis of Diketo Esters 5 and 7. Sodium ethoxide (390 mg, 5.5 mmol) was added into a well-stirred mixture of **9** or **10** (2.7 mmol) and diethyl oxalate (790 mg, 5.4 mmol) in anhydrous THF (2.7 mL) under nitrogen atmosphere. The mixture was stirred at room temperature (2 h for **5**, 45 min for **7**) and then was poured into *n*-hexane (50 mL). The collected precipitate was vigorously stirred for 30 min in 1 N HCl (50 mL). The yellow solid that formed was filtered, washed with water, and dried under an IR lamp. **5**: 100% yield; mp >300 °C (DMF/water). Anal. ($C_{21}H_{19}NO_9$) C, H, N. **7**: 88% yield; mp 189−190 °C (toluene). Anal. ($C_{28}H_{24}FNO_9$) C, H, N, F.

General Procedure for the Synthesis of Diketo Acids 6 and 8. A mixture of 1 N NaOH (6.5 mL) and compound **5** or **7** (1.3 mmol) in THF/methanol 1:1 (12 mL) was stirred at room temperature for 18 h and then poured onto crushed ice. The aqueous layer was separated and treated with 1 N HCl until reaching pH 3, and the yellow solid that formed was collected by filtration and then washed with water, hot dry ethanol, and light petroleum ether. **6**: 52% yield; mp >300 °C (washed with hot acetone). Anal. ($C_{17}H_{11}NO_9$) C, H, N. **8**: 77% yield; mp 178−180 °C (washed with hot dry ethanol). Anal. ($C_{24}H_{16}FNO_9$) C, H, N, F.

Biological Assays. Integrase Assays. Compounds **5**−**8** were tested for their ability to inhibit HIV-1 integrase in vitro using a gel-based assay in addition to a plate-based electrochemiluminescent assay.

In the gel assay, a 5′-end-labeled 21-mer double-stranded DNA oligonucleotide, corresponding to the last 21 bases of the U5 viral LTR, is used to follow both the 3′-processing and strand transfer steps of the integration reaction (for review, see ref 6). Briefly, a DNA−enzyme complex is preformed by mixing 500 nM of recombinant HIV-1 integrase and 20 nM of 5′-labeled double-stranded DNA template in a buffer containing 50 mM MOPS, pH 7.2, 7.5 mM $MnCl_2$ or $MgCl_2$, and 14.3 mM β-mercaptoethanol for 15 min on ice. The integration reaction is then initiated by addition of the drug and continued in a total volume of 10 μL for 60 min at 37 °C. The reaction samples are stopped by adding the same volume of electrophoresis denaturing dye and loaded on 20% 19/1 acrylamide denaturing gel. Gels were exposed overnight and analyzed using a Molecular Dynamics Phosphorimager (Sunnyvale, CA).

The plate-based electrochemiluminescent assay was performed using a BioVeris M-SERIES Analyzer (Gaithersburg, MD). DNA substrates were obtained from BioVeris and used according to the manufacturer's recommendations. Briefly, donor DNA is incubated for 30 min at 37 °C in the presence of 250 nM of recombinant HIV-1 integrase. After addition of the drug, the integration reaction is initiated by addition of target DNA. Reaction is carried out for 60 min at 37 °C and then read on the BioVeris M-SERIES Analyzer.

Anti-HIV Assays in Cultured Cell Lines. The anti-HIV drug testing was performed in 96-well plates with a defined, previously titered inoculum of a laboratory strain (HTLV-IIIB) to minimize the inoculum effect.

In brief, all compounds were dissolved in dimethyl sulfoxide and diluted in cell culture medium at concentrations ranging from 0.1 to 50 μM. Exponentially growing human T lymphocytes (H9 cell line) were added at 5000 cell/well. After the infectivity of a virus stock (HTLV-IIIB) was quantified, an aliquot containing 1×10^5 50% tissue culture infectious dose ($TCID_{50}$) per 5000 H9 cells per well is used as inoculum in each set of in vitro infections of H9 cells. Uninfected cells with the compound served as a toxicity control, and infected and uninfected cells without the compound served as basic controls. Cultures were incubated at 37 °C in a 5% CO_2 atmosphere for 4 days. Supernatant fluid of infected wells (in the absence of drug and at each of a number of drug concentrations) was harvested. HIV p24 antigen was quantified and the 50%

inhibitory concentration (IC_{50}) of drug was determined using the median effect equation.

Cytotoxicity Assays. The cytotoxicity of test compounds was evaluated on human histiocytic lymphoma (U937) cell line obtained from the American Type Culture Collection (ATCC, Rockville, MD). Cells were plated in a 96 well-plate at a concentration of 5×10^3/mL in RPMI-1640 without phenol red, supplemented with 20% fetal calf serum and antibiotics. Two hours after plating, compounds were added at different concentrations ranging from 1 μg/mL to 200 mg/mL and cells were incubated at 37 °C for 24 h. Then, cells were incubated at 37 °C for 3 h with 1 mg/mL of MTT (Sigma-Aldrich, Milan, Italy). After incubation, the remaining water-insoluble formazan was solubilized in absolute 2-propanol containing 0.1 N HCl. Absorbance of converted dye was measured in an ELISA plate reader at the wavelength of 570 nm. The cytotoxicity of the compounds was calculated as the percentage reduction of the viable cells compared with the drug-free control culture. The drug concentration required to reduce the cell viability by 50% is called IC_{50}.

Molecular Modeling. Molecular Dynamics (MD) Simulation. The catalytic core domain (CCD) structure of HIV-1 integrase (IN) was taken from PDB structure 1BIS.[17] The chain B of the X-ray structure was chosen for our studies, and a Mg^{2+} ion was placed in the active site between the carboxylate oxygen atoms of amino acid residues D64 and D116 considering the geometry of the Mg^{2+} ion that was present in the subunit A of the PDB structure 1QS4.[18] To sample the conformational space of IN enzyme, a 1-ns MD simulation was carried out in explicit solvent. All the water molecules present in the X-ray structure of the enzyme were removed and all hydrogen atoms were added to the residues, considering residues Arg, Lys, Glu, and Asp in their charged form, while all His residues were considered neutral by default. To make the system electroneutral, a total of two neutralizing counterions (Cl^-) were added with the aid of the program VEGA (v 1.5.0).[27] The enzyme was then soaked with a 10 Å water layer. The calculations were carried out with the DISCOVER module of the INSIGHT II program using the CVFF force field.[28] A multiple-step procedure was used. The complex was energetically minimized with 5000 steps of a steepest descent minimization, followed by 3000 steps of conjugate gradient minimization to adjust the water molecules and the counterions locally and to eliminate any residual geometrical strain, while the heavy atoms of the enzyme were kept fixed. The minimized solvated system was used as the initial structure for an equilibration stage (100 ps), followed by a production run (1 ns). In the equilibration stage, energy minimization of the protein side chains was achieved by employing 5000 steps of steepest descent and 3000 steps of conjugate gradient algorithm. The system was then heated gradually starting from 10 to 300 K in 5-ps steps and was equilibrated with temperature bath coupling (300 K). During the equilibration and the production run, the backbone of the enzyme secondary structures was kept fixed. A cutoff of 13 Å was used for nonbonded interactions. Coordinates and energies were saved every 10 ps, yielding 100 structures. For the purpose of automatic docking, a snapshot was taken each 100 ps.

Docking Simulations. Docking of **8** to IN CCD was carried out using the AutoDock program package version 3.0.5.[20] The LGA algorithm, as implemented in the AutoDock program, applied a protocol with a maximum number of 1.5×10^{-6} energy evaluations, a mutation rate of 0.01, a crossover rate of 0.80, and an elitism value of 1. For the local search, the pseudo-Solis and Wets algorithm was applied using a maximum of 300 interactions per local search. Fifty independent docking runs in different enzyme MD snapshots were carried out for **8**. Results differing by less than 1.5 Å in positional root-mean-square deviation were clustered together and represented by the result with the most favorable free energy of binding. The obtained complexes were energetically minimized using 3000 steps of steepest descent algorithm, while only the ligand and the side chain atoms of the protein within a radius of 5 Å around the ligand were permitted to relax. The geometry optimization was carried out employing the DISCOVER program with the CVFF force field.

(**1**) **Ligand Setup.** The structure of **8** was generated from the standard fragment library of the SYBYL software version 7.0.[29] Geometry optimizations were achieved with the SYBYL/MAXIMIN2 minimizer by applying the BFGS algorithm[30] with a convergence criterion of 0.001 kcal/mol and by employing the TRIPOS force field. Partial atomic charges were assigned using the Gasteiger and Marsili formalism[31] as implemented in the SYBYL package. **8** was modeled in its keto−enolic form with the negatively charged carboxylate groups. Six flexible torsions were specified: two around the quinoline ring, two about the benzyl group, and two allowing the hydroxyl groups to rotate.

(**2**) **Protein Setup.** The protein structure was set up for docking as follows: the unpolar hydrogens were removed and Kollman united-atom partial charges were assigned. Solvation parameters were added to the protein−DNA complex using the ADDSOL utility of the AutoDock program. The grid maps were calculated with AutoGrid. The grids were chosen to be large enough to include a significant part of the protein around the catalytic site. In all cases, we used grid maps with $61 \times 61 \times 61$ points with a grid-point spacing of 0.375 Å. The center of the grid was set to be coincident with the Mg^{2+} ion in the active site of catalytic domain.

Acknowledgment. The authors thank Prof. J. Andrew McCammon for the donation of the IN−DNA complex coordinates. We also thank Dr. M. Zancato (University of Padova, Italy) for performing elemental analyses. This project was supported by Ministero della Sanità, Istituto Superiore di Sanità, "Programma Nazionale di ricerca sull' AIDS" (Grant No. 30F.19), Italian MIUR (PRIN 2004), and in part by the Center for Cancer Research, National Cancer Institute, National Institutes of Health.

Supporting Information Available: Spectroscopic data for compounds **5**−**10**, elemental analyses for derivatives **5**−**8**, and details of the docking setup and the MD simulation protocol. This material is available free of charge via the Internet at http://pubs.acs.org.

References

(1) Hammer, S. M. Clinical practice. Management of newly diagnosed HIV infection. *N. Engl. J. Med.* **2005**, *353*, 1702−1710.
(2) Cohen, J. Therapies. Confronting the limits of success. *Science* **2002**, *296*, 2320−2324.
(3) Fesen, M. R.; Kohn, K. W.; Leteurtre, F.; Pommier, Y. Inhibitors of human immunodeficiency virus integrase. *Proc. Natl. Acad. Sci. U.S.A.* **1993**, *90*, 2399−2403.
(4) Cushman, M.; Sherman, P. Inhibition of HIV-1 integration protein by aurintricarboxylic acid monomers, monomer analogs, and polymer fractions. *Biochem. Biophys. Res. Commun.* **1992**, *185*, 85−90.
(5) Carteau, S.; Mouscadet, J.-F.; Goulaouic, H.; Subra, F.; Auclair, C. Inhibitory effect of the polyanionic drug suramin on the in vitro HIV DNA integration reaction. *Arch. Biochem. Biophys.* **1993**, *305*, 606−610.
(6) Pommier, Y.; Johnson, A. A.; Marchand, C. Integrase inhibitors to treat HIV/AIDS. *Nat. Rev. Drug Discovery* **2005**, *4*, 236−248.
(7) Johnson, A. A.; Marchand, C.; Pommier, Y. HIV-1 integrase inhibitors: A decade of research and two drugs in clinical trial. *Curr. Top. Med. Chem.* **2004**, *4*, 1059−1077.
(8) Hazuda, D. J.; Felock, P.; Witmer, M.; Wolfe, A.; Stillmock, K.; Grobler, J. A.; Espeseth, A.; Gabryelski, L.; Schleif, W.; Blau, C.; Miller, M. D. Inhibitors of strand transfer that prevent integration and inhibit HIV-1 replication in cells. *Science* **2000**, *287*, 646−650.
(9) Wai, J. S.; Egbertson, M. S.; Payne, L. S.; Fisher, T. E.; Embrey, M. W.; Tran, L. O.; Melamed, J. Y.; Langford, H. M.; Guare, J. P., Jr.; Zhuang, L.; Grey, V. E.; Vacca, J. P.; Holloway, M. K.; Naylor-Olsen, A. M.; Hazuda, D.; Felock, P. J.; Wolfe, A. L.; Stillmock, K. A.; Schleif, W. A.; Gabryelski, L. J.; Young, S. D. 4-Aryl-2,4-dioxobutanoic acid inhibitors of HIV-1 integrase and viral replication in cells. *J. Med. Chem.* **2000**, *43*, 4923−4926.

(10) Espeseth, A.; Felock, P.; Wolfe, A.; Witmer, M.; Grobler, J. A.; Anthony, N.; Egbertson, M.; Melamed J. Y.; Young, S.; Hamill, T.; Cole, J. L.; Hazuda, D. J. HIV-1 integrase inhibitors that compete with the target DNA substrate define a unique strand transfer conformation for integrase. *Proc. Natl. Acad. Sci. U.S.A.* **2000**, *97*, 11244−11249.
(11) Grobler, J. A.; Stillmock, K.; Hu, B.; Witmer, M.; Felock, P.; Espeseth, A. S.; Wolfe, A.; Egbertson, M.; Bourgeois, M.; Melamed, J.; Wai, J. S.; Young, S.; Vacca, J.; Hazuda, D. J. Diketo acid inhibitor mechanism and HIV-1 integrase: Implications for metal binding in the active site of phosphotransferase enzymes. *Proc. Natl. Acad. Sci. U.S.A.* **2002**, *99*, 6661−6666.
(12) Marchand, C.; Johnson, A. A.; Karki, R. G.; Pais, G. C.; Zhang, X.; Cowansage, K.; Patel, T. A.; Nicklaus, M. C.; Burke, T. R., Jr.; Pommier, Y. Metal-dependent inhibition of HIV-1 integrase by beta-diketo acids and resistance of the soluble double-mutant (F185K/C280S). *Mol. Pharmacol.* **2003**, *64*, 600−609.
(13) Marchand, C.; Zhang, X.; Pais, G. C. G.; Cowansage, K.; Neamati, N.; Burke, T. R., Jr.; Pommier Y. Structural determinants for HIV-1 integrase inhibition by β-diketo acids. *J. Biol. Chem.* **2002**, *277*, 12596−12603.
(14) Pais, G. C. G.; Zhang, X.; Marchand, C.; Neamati, N.; Cowansage, K.; Svarovskaia, E. S.; Pathak, V. K.; Tang, Y.; Nicklaus, M.; Pommier Y.; Burke, T. R., Jr. Structure activity of 3-aryl-1,3-diketo-containing compounds as HIV-1 integrase inhibitors. *J. Med. Chem.* **2002**, *45*, 3184−3194.
(15) Long, Y.-Q.; Jiang, X.-H.; Dayam, R.; Sanchez, T.; Shoemaker, R.; Sei, S.; Neamati, N. Rational design and synthesis of novel dimeric diketoacid-containing inhibitors of HIV-1 integrase: Implication for binding to two metal ions on the active site of integrase. *J. Med. Chem.* **2004**, *47*, 2561−2573.
(16) (a) Artico, M.; Di Santo, R.; Costi, R.; Novellino, E.; Greco, G.; Massa, S.; Tramontano, E.; Marongiu, M. E.; De Montis, A.; La Colla, P. Geometrically and conformationally restrained cinnamoyl-compounds as inhibitors of HIV-1 integrase: Synthesis, biological evaluation and molecular modeling. *J. Med. Chem.* **1998**, *41*, 3948−3960. (b) Di Santo, R.; Costi, R.; Artico, M.; Tramontano, E.; La Colla, P.; Pani, A. HIV-1 integrase inhibitors that block HIV-1 replication in infected cells. Planning synthetic derivatives from natural products. *Pure Appl. Chem.* **2003**, *75*, 195−206. (c) Costi, R.; Di Santo, R.; Artico, M.; Massa, S.; Ragno, R.; Loddo, R.; La Colla, M.; Tramontano, E.; La Colla, P.; Pani. A. 2,6-Bis(3,4,5-trihydroxybenzylidene) derivatives of cyclohexanone: Novel potent HIV-1 integrase inhibitors that prevent HIV-1 multiplication in cell-based assays. *Bioorg. Med. Chem.* **2004**, *12*, 199−215. (d) Costi, R.; Di Santo, R.; Artico, M.; Roux, A.; Ragno, R.; Massa, S.; Tramomtano, E.; La Colla, M.; Loddo, R.; Marongiu, M. E.; Pani, A.; La Colla, P. 6-Aryl-2,4-dioxo-5-hexenoic acids, novel integrase inhibitors active against HIV-1 multiplication in cell-based assays. *Bioorg. Med. Chem. Lett.* **2004**, *14*, 1745−1749. (e) Di Santo, R.; Costi, R.; Artico, M.; Ragno, R.; Greco, G.; Novellino, E.; Marchand, C.; Pommier, Y. Design, synthesis and biological evaluation of heteroaryl diketohexenoic and diketobutanoic acids as HIV-1 integrase inhibitors endowed with antiretroviral activity. *Il Farmaco* **2005**, *60*, 409−417.
(17) Goldgur, Y.; Dyda, F.; Hickman, A. B.; Jenkins, T. M.; Cragie, R.; Davies, D. R. Three new structure of the core domain of HIV-1 integrase: An active site that binds magnesium. *Proc. Natl. Acad. Sci. U.S.A.* **1998**, *95*, 9150−9154.
(18) Goldgur, Y.; Craigie, R.; Cohen, G. H.; Fujiwara, T.; Yoshinaga, T.; Fujishita, T.; Sugimoto, H.; Endo, T.; Murai, H.; Davies, D. R. Structure of the HIV-1 integrase catalytic domain complexed with an inhibitor: A platform for antiviral drug design. *Proc. Natl. Acad. Sci. U.S.A.* **1999**, *96*, 13040−13043.
(19) Lin, J.-H.; Perryman, A. L.; Schames, J. R.; McCammon, J. A. Computational drug design accommodating receptor flexibility: The relaxed complex scheme. *J. Am. Chem. Soc.* **2002**, *124*, 5632−5633.
(20) Morris, G. M.; Goodsell, D. S.; Halliday, R. S.; Huey, R.; Hart, W. E.; Belew, R. K.; Olson, A. J. Automated docking using a lamarckian genetic algorithm and an empirical binding free energy function. *J. Comput. Chem.* **1998**, *19*, 1639−1662.
(21) Greenwald, J.; Le, V.; Butler, S. L.; Bushman, F. D.; Choe, S. The mobility of an HIV-1 integrase active site loop is correlated with catalytic activity. *Biochemistry* **1999**, *38*, 8892−8898.
(22) Lins, R. D.; Briggs, J. M.; Straatsma, T. P.; Carlson, H. A.; Greenwald, J.; Choe, S.; McCammon, J. A. Molecular dynamics studies on the HIV-1 integrase catalytic domain. *Biophys. J.* **1999**, *76*, 2999−3011.
(23) Podtelezhnikov, A. A.; Gao, K.; Bushman, F. D.; McCammon, J. A. Modeling HIV-1 integrase complexes based on their hydrodynamic properties. *Biopolymers* **2003**, *68*, 110−120.
(24) van Gent, D. C.; Groeneger, A. A.; Plasterk, R. H. Mutational analysis of the integrase protein of human immunodeficiency virus type 2. *Proc. Natl. Acad. Sci. U.S.A.* **1992**, *20*, 9598−9602.
(25) Jenkins, T. M.; Esposito, D.; Engelman, A.; Cragie, R. Critical contacts between HIV-1 integrase and viral DNA identified by structure-based analysis and photo-crosslinking. *EMBO J.* **1997**, *16*, 6849−6859.
(26) Coates, R. M.; Hobbs, S. J. α-Alkoxyallylation of activated carbonyl compounds. A novel variant of the Michael reaction. *J. Org. Chem.* **1984**, *49*, 140−152.
(27) Pedretti, A.; Villa, L.; Vistoli, G. VEGA: A versatile program to convert, handle, and visualize molecular structure on Windows based PCs. *J. Mol. Graph.* **2002**, *21*, 47−49.
(28) Accelrys, 2001, San Diego, CA.
(29) SYBYL Molecular Modeling System, TRIPOS Assoc., St. Louis, MO.
(30) Head, J.; Zerner, M. C. A Broyden−Fletcher−Goldfarb−Shanno optimization procedure for molecular geometries. *Chem. Phys. Lett.* **1985**, *122*, 264−274.
(31) Gasteiger, J.; Marsili, M. Iterative partial equalization of orbital electronegativity−A rapid access to atomic charges. *Tetrahedron* **1980**, *36*, 3219−3228.

JM0511583